BENEFITS OF SATURATION PROFILES FOR ESTIMATING GAS AND LIQUID RELATIVE PERMEABILITIES FROM CENTRIFUGE TESTS

Osamah Al-Omair (Kuwait University) and
Richard L. Christiansen (Colorado School of Mines)

ABSTRACT

In conventional centrifuge tests, the relative permeability of just one phase is obtained – the phase with the lowest mobility. As a result, centrifuge tests are most often used for obtaining relative permeabilities of a liquid in a gas-liquid pair. In order to obtain more relative permeability insight from a centrifuge test, data in addition to production data must be obtained. In this paper, we discuss measurements of evolving air-water saturation profiles for a spinning-disk geometry. The saturation profiles were obtained by processing video images of the spinning rock sample, which was held in a transparent rotor assembly. Relative permeabilities of the water and the air were obtained by history-matching the saturation profiles and the production data. Critical gas saturation can be approximately estimated from the saturation profiles. In addition to the relative permeability results, we show a comparison of capillary pressures measured with the centrifuge (standard geometry and the spinning disk geometry), with a porous plate, and with mercury injection. For one of the samples, all four methods agreed well. For most samples, the centrifuge and the porous-plate methods agreed well.

INTRODUCTION

Capillary pressure and relative permeabilities are essential for understanding and predicting movement of multiple phases in petroleum reservoirs. These properties are measured with a variety of laboratory techniques, including porous plate, mercury injection, and centrifuge methods for capillary pressure, and displacements at normal gravitational acceleration and in the centrifuge for relative permeabilities. Centrifuge methods are increasingly used for a number of reasons, including short duration of the tests, and the potential for measurements near end-point saturations. Measurements of relative permeabilities with a centrifuge are generally limited to fluids of high mobility contrast (gas & liquid, water & heavy oil). Indeed, just the relative permeability of the low mobility fluid can be obtained from standard tests.[1]

The limitation of the centrifuge method for relative permeability measurement results from its "narrow" data set: the typical data set is a list of fluids produced as a function of time for one or more spin rates. A displacement at normal gravitational acceleration for measurement of relative permeabilities does not suffer the same limitation because its data set is broad: it includes pressure drop and production data as a function of time, and sometimes saturation distributions measured with CT-Scanning and other methods. Clearly, the status of centrifuge methods could be grossly improved by incorporating techniques that broaden the data set.

To broaden the data set for centrifuge tests, instrumentation must cope with a rapidly spinning rotor. This is not an insurmountable obstacle. In 1988, Firoozabadi *et al*.[2] described a centrifuge with means for adding or removing fluids to the sample chamber on the rotor through a rotating seal in response to changes in resistivity around a probe in the chamber. Chardaire-Riviere *et al*.[3] mounted three ultrasonic transducers along the length of a rock sample in order to monitor saturation changes. Pohjoisrinne *et al*.[4] measured fluid level in a spinning bucket with a capacitative method and passed data to the non-spinning world with infrared transmissions.

In the remainder of this paper, we discuss our experiences with measurement of saturation profiles with video imaging to obtain gas and liquid relative permeabilities using the spinning-disk geometry in a centrifuge. As a side note, results of capillary pressure measurements with four different methods are compared at the end of the paper.

DESCRIPTION OF LABORATORY METHODS

The spinning-disk geometry[5] is particularly suited for video measurement of saturation profiles because the cylindrical rock sample spins on its axis. Thus, a standard video camera can capture images of the spinning sample without concern for synchonization that would be needed in the conventional centrifuge geometry. The sample holder is shown in Figures 1 and 2. The sample holder was made of clear polycarbonate to allow viewing of the rock sample enclosed in the holder. In this implementation of the spinning-disk geometry, the produced liquid collects in the cylindrical gap above the rock sample and in the rectangular fluid collection channel below the sample. As a result, the gas-liquid interface is always in contact with the rock sample, providing a clear definition of the radius of zero capillary pressure. This mode of fluid collection is similar to that described by Oyno and Torsaeter[6] and it provides for study of the spontaneous imbibition process – we will not discuss those results here.

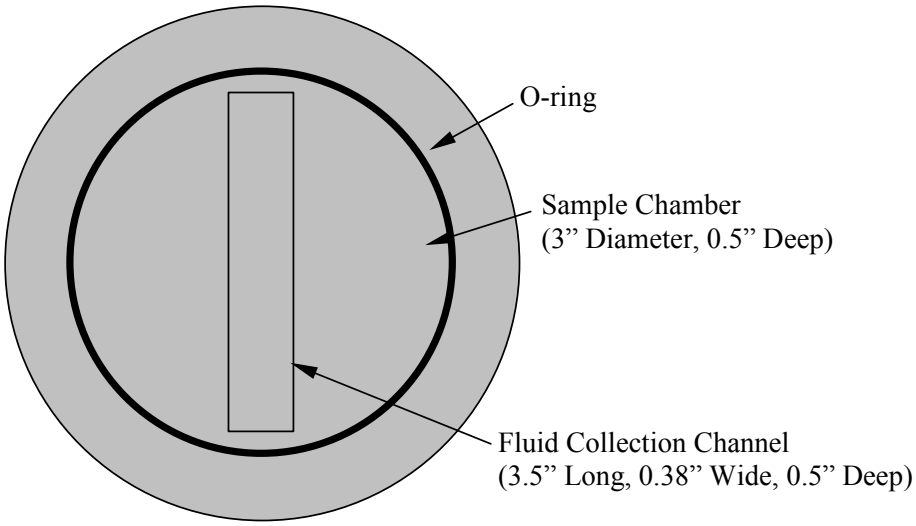

Figure 1. Top-view of sample holder.

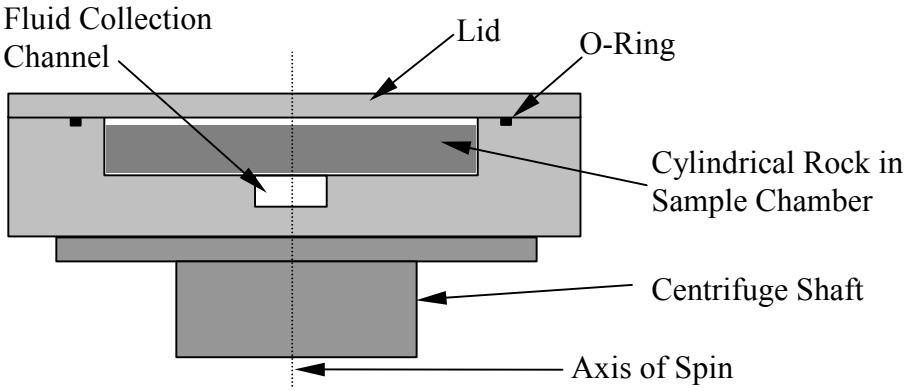

Figure 2. Side-view of sample holder attached to the shaft of the centrifuge.

During the spinning-disk tests, black-and-white video images of the rock sample and the produced fluid were continuously recorded. The fluid production was measured from the sample image by locating the radius of the gas-brine interface that contacts the rock. The local saturation was obtained from the video image by a correlation that relates the gray level to the saturation. (See Al-Omair[7] for details.) With the visualizing method, we were able to measure saturation profiles and drainage and spontaneous imbibition capillary pressure relationships for ten samples of rock. Results for five of these samples (described in Table 1) are presented in this paper.

We have used the video method for several different studies of saturation distributions in porous materials. This method is inexpensive to employ, but it perceives just the saturation at the surface of the sample, unless the sample is transparent. If the surface of the sample must be sealed to satisfy a boundary condition, then the video method is difficult if not impossible to apply. Unfortunately, we would like to have the two flat sides of the cylindrical rock sample sealed for measurements of relative permeability. As sealing would prohibit the use of the video method, we chose to sacrifice the boundary condition. This means that the relative permeabilities that we observe are not quantitatively correct. However, we believe that our results clearly demonstrate the value of saturation profile data for obtaining relative permeabilities.

Table 1. Properties of Rock Samples.

Sample	Type	Diameter, cm	Thickness, cm	Porosity	Permeability, md
1D	Dolomite	8.3	1.2	9.8	70.2
2D	Berea	8.3	1.2	24.3	6400
4D	Berea	8.3	1.2	22.6	953
6D	Berea	8.3	1.2	15.5	1280
9D	Berea	8.3	1.3	20.5	125

ANALYSIS OF DATA

Two numerical tools were used for obtaining relative permeability data from the centrifuge tests. First, a numerical model of the gas-liquid displacement in the spinning-disk was used to match the history of liquid production and the movement of saturation profiles. Second, the prediction of movement of saturation profiles as presented by Hagoort gave insight for estimating the critical gas saturation. These approaches are needed because the large variation in centrifugal acceleration in our spinning-disk tests precludes differentiation of production data to obtain relative permeabilities.

The numerical model uses an IMPES (implicit pressure, explicit saturation) finite-difference scheme to sequentially solve the differential pressure and saturation equations. The differential equations are obtained by combining a one-dimensional radial material balance with Darcy's law modified to include relative permeabilities. Relative permeabilities were represented with modified Brooks-Corey expressions.

$$k_{rw} = k_{rw,\max}\left(\frac{S_w - S_{wi}}{1 - S_{wi} - S_{gc}}\right)^{nw} \tag{1}$$

$$k_{rg} = k_{rg,\max}\left(\frac{S_g - S_{gc}}{1 - S_{wi} - S_{gc}}\right)^{ng} \tag{2}$$

In these empirical expressions, S_{wi} is the irreducible water saturation, S_{gc} is the critical gas saturation, nw and ng are power-law exponents, and $k_{rw,max}$ and $k_{rg,max}$ are the maximum relative permeabilities for water and gas. Both power-law and Bentsen-Anli expressions were used for capillary pressure. In the model, the flat surfaces of the rock sample were treated as non-flow boundaries. However, fluids could pass through the center node and the outside circular edge of the radial model. These boundary conditions are not identical to those in the experiments, in which none of the surfaces were sealed. Although we recognize that the differences in the boundary conditions affect the quantitative interpretation of the experiments with the model, we hope that our analysis sufficiently demonstrates the value of saturation profile data for measuring relative permeabilities in centrifuge tests. (See Al-Omair[7] for details.) A two-dimensional radial model could improve interpretation of the experiments by incorporating boundary conditions that are more similar to the experiment.

The second tool is the expression for the saturation profile during the displacement as developed by Hagoort for the standard centrifuge geometry:

$$r_{Sw} = \frac{\Delta\rho\alpha k k'_{rw} t}{\phi\mu_w} + r_i \tag{3}$$

In this expression,

r_{Sw} = the radial position of water saturation S_w;
$\Delta\rho$ = the gas-water density difference;
α = the centrifugal acceleration at the sample mid-point;
k = the absolute permeability;
k'_{rw} = the derivative with respect to water saturation of k_{rw} at S_w;
t = time;
μ_w = viscosity of water;
r_i = radius at inside face of rock sample.

Applying Eq. 3, the saturation at the displacement front must equal the critical gas saturation because lower gas saturations will not propagate. A saturation profile constructed with Eq. 3 for a critical gas saturation of 0.10 is shown in Figure 3. (See Christiansen[8] for details, including software.)

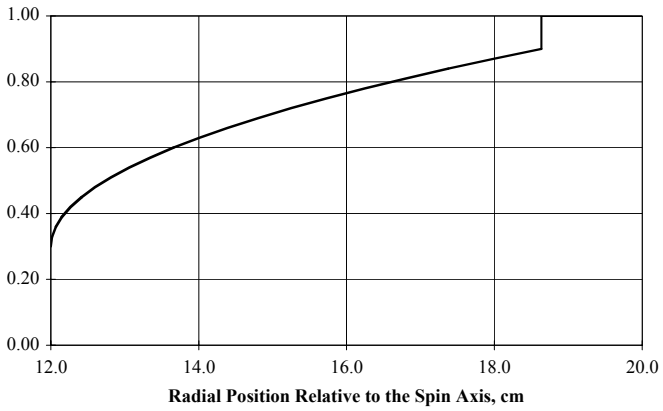

Figure 3. A water saturation profile constructed with Eq. 3 for a gas-water displacement in the standard centrifuge geometry. The height of the shock equals the critical gas saturation.

Several cautions should be observed for application of Eq. 3 for interpretation of real saturation profiles. First, an actual displacement front will be smeared by capillary effects; nevertheless, the critical gas saturation can be estimated from the saturation profile. Second, one must be careful to use profiles from the early portion of a centrifuge test. In latter portions of the test, the saturation profile asymptotically approaches an equilibrium distribution. For example, the saturation profiles at 1000 sec and 2200 sec in Figure 4 give a satisfactory estimate of the critical gas saturation (about 11%), while profiles at later times do not have a well-defined front because they are approaching the equilibrium saturation profile. Third, Eq. 3 is strictly correct for the tradition centrifuge geometry; it is only qualitatively applicable to our spinning-disk geometry.

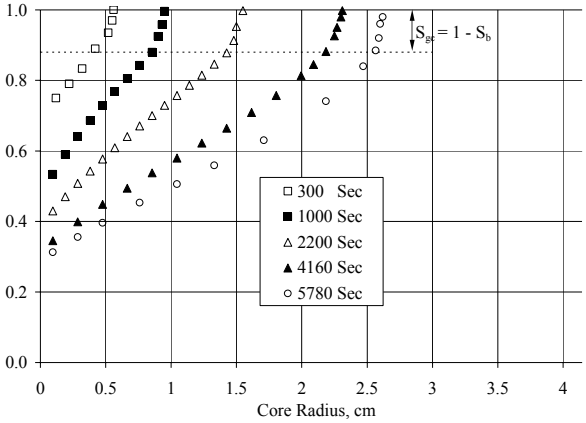

Figure 4. Saturation profiles for Sample 4D spinning at 1800 rpm.

RESULTS FOR GAS AND LIQUID RELATIVE PERMEABILTY

The capillary pressure behavior in the numerical model was adjusted to fit the equilibrium saturation profile obtained from the video record of a sample. Then, estimates of the gas and liquid relative permeabilities were obtained by fitting the model to production data such as shown in Figure 5. The resulting relative permeabilities in Figure 6 depend on the spin rate – an undesirable result. The large variation in gas relative permeabilities reflects the insensitivity of water production to gas relative permeability. The variation in water relative permeabilities with spin rate is also large, although it is not as large as that for gas.

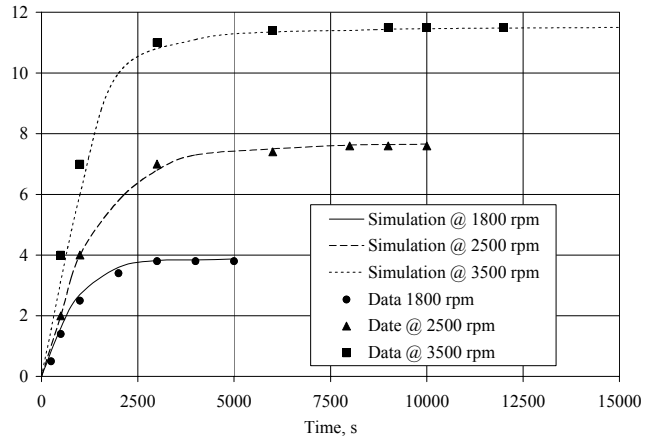

Figure 5. Production data and history matches for Sample 4D.

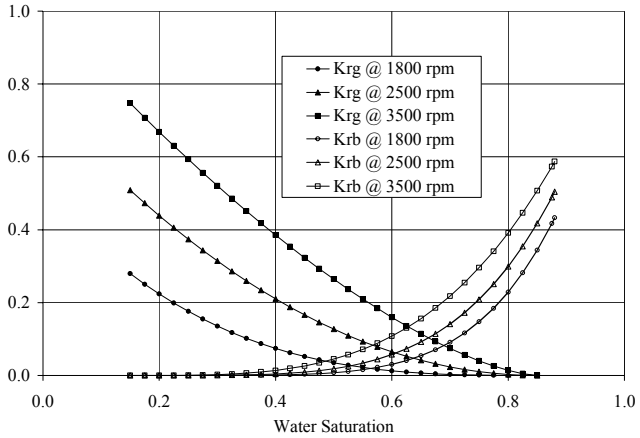

Figure 6. Relative permeabilities from matching production histories at different spin rates for Sample 4D.

The variation in relative permeabilities is eliminated for Sample 4D when the relative permeability parameters in the numerical simulator are adjusted to match both the production data and the saturation profiles collected with the video imaging technique as shown in Figure 7. Critical gas saturations for the relative permeability models were estimated from the slight kink at the front of the saturation profiles as described in a previous section. Irreducible water saturations were obtained from the capillary pressure measurements. Consequently, just the maximum relative permeabilities and the exponents in Eqs. 1 and 2 were adjusted during the fitting process. The saturation profiles and the match for two spin rates are shown in Figures 8 and 9. Another example of the benefit of saturation profiles is shown in Figures 10 and 11 for Sample 9D.

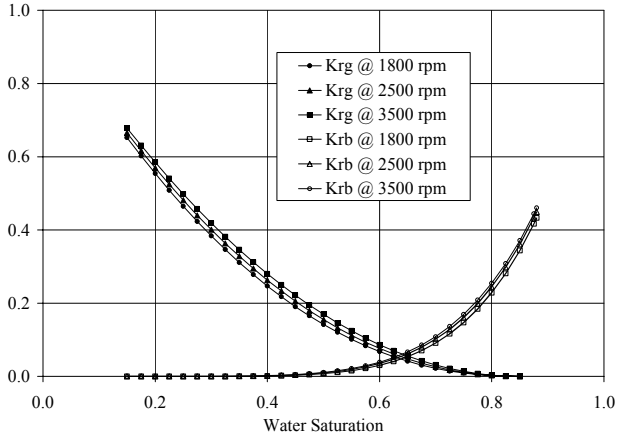

Figure 7. Relative permeabilities from a combined match of water production and saturation profiles for Sample 4D.

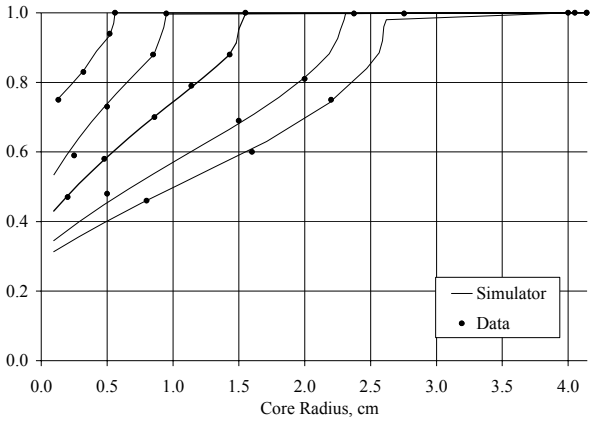

Figure 8. Measured and matched saturation profiles for Sample 4D at 1800 rpm.

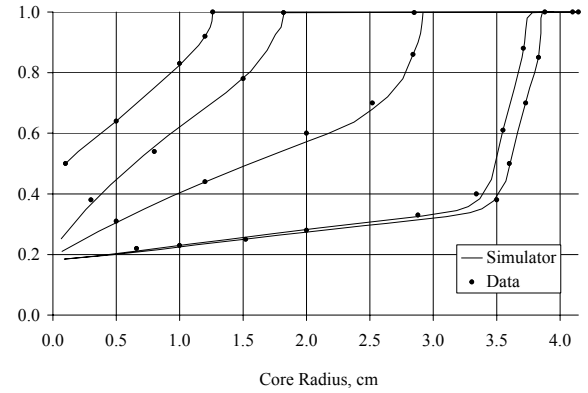

Figure 9. Measured and matched saturation profiles for Sample 4D at 3500 rpm.

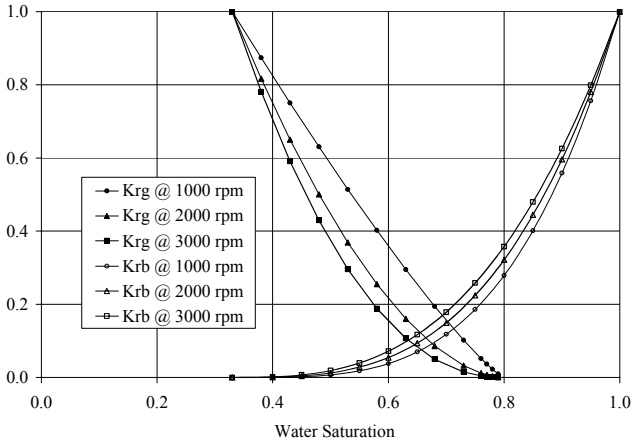

Figure 10. Relative permeabilities from matching production histories at different spin rates for Sample 9D.

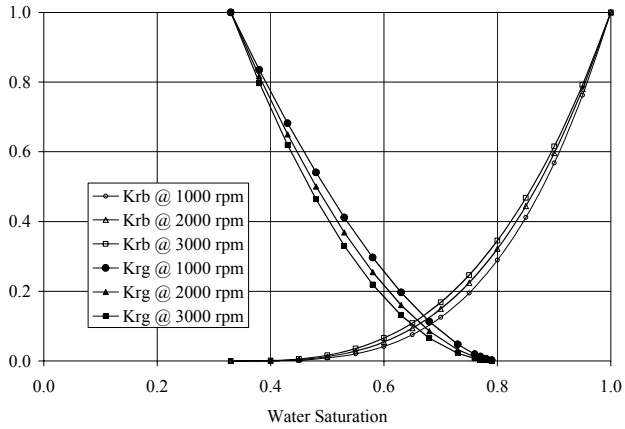

Figure 11. Relative permeabilities from a combined match of water production and saturation profiles for Sample 9D.

COMPARISON OF CAPILLARY PRESSURES

The emphasis of this paper is measurement of relative permeabilities with centrifuge methods. Yet, we made many measurements of capillary pressure during our study as a means for increasing confidence in our ability to make accurate measurements of fluid saturations with the video method. We share some of these results here for two reasons. First, they demonstrate the quality of our capillary pressure data, which is integral to the history-matching process for obtaining relative permeabilties. And second, the comparison of capillary pressures from four different methods is thought provoking.

Capillary pressure relationships were measured with four methods: mercury injection, porous-plate, standard geometry, spinning-disk geometry. The Hassler-Brunner method was used to process the data from the centrifuge tests with the standard geometry. The data from the spinning-disk geometry were processed in a manner used previously (Al-Omair and Christiansen[9]). In short, the saturation at any radius in the sample was found by correlation of the video gray level with saturation. The capillary pressure at that radius was calculated with Eq. 4:

$$P_c(r,\omega) = \frac{1}{2}\Delta\rho\omega^2\left(R_{gw}{}^2 - r^2\right) \qquad (4)$$

This method is analogous to that used by Spinler and Baldwin[10] for obtaining capillary pressure relationships from NMR measurements on samples taken from a centrifuge.

The results of capillary pressure measurements for three of six samples are shown in Figures 12 to 14. These figures show that results from the porous-plate method, and both centrifuge methods are in fairly good agreement. However, the results for mercury injection (adjusted for comparison to the gas-water by dividing the capillary pressure by 5.1) differ qualitatively from the other results in Figures 12 and 13. Of the six samples for

which comparative results were obtained, Sample 6D was the only one for which all methods gave similar results as shown in Figure 14. This result may be surprising to many reservoir engineers who use the following expression for adjusting capillary pressure measurements from laboratory (L) to reservoir (R) conditions:

$$\frac{P_{cR}}{P_{cL}} = \frac{(\sigma \cos\theta)_R}{(\sigma \cos\theta)_L} \tag{5}$$

Its wide-spread use suggests that Equation 5 works quite well at times, although it failed for most of our samples.

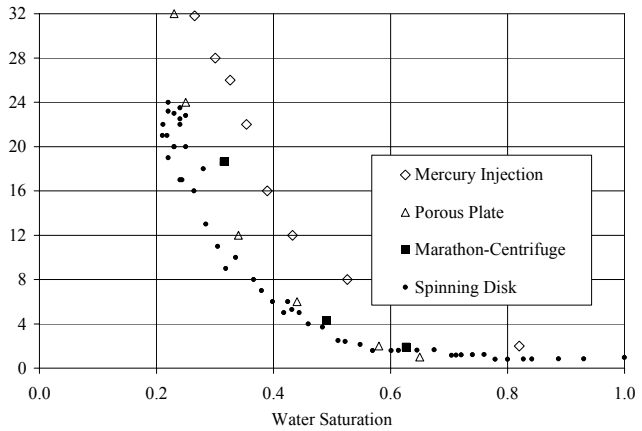

Figure 12. Comparison of capillary pressure results for Sample 1D.

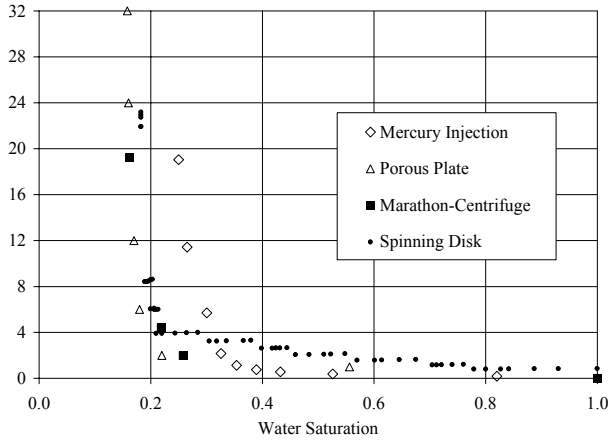

Figure 13. Comparison of capillary pressure results for Sample 2D.

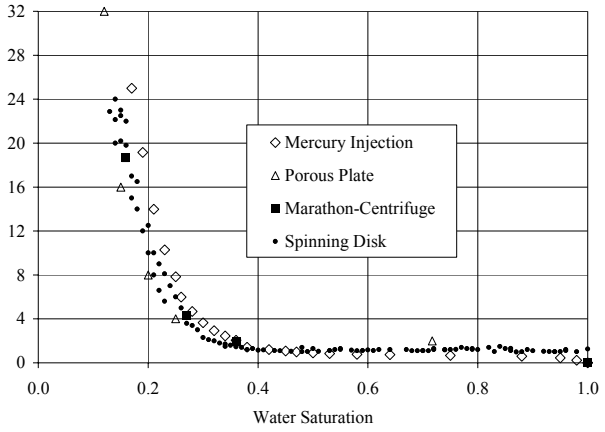

Figure 14. Comparison of capillary pressure results for Sample 6D.

CONCLUSIONS

1. Liquid relative permeability relationships can be obtained from spinning-disk tests by matching production history.

2. Gas relative permeability relationships cannot be obtained with any certainty through analysis of just the production data from centrifuge tests.

3. Combining saturation profile data with production data from centrifuge tests reduces the uncertainty in the relative permeability relationships for both gas and liquid.

4. Critical gas saturation can be estimated from the shape of the saturation profile in centrifuge tests during the drainage process.

5. For the spinning-disk geometry, there is no data-reduction scheme similar to that of Hagoort for the traditional centrifuge geometry.

6. Capillary pressure relationships obtained from spinning-disk tests are in good agreement with those obtained from traditional centrifuge tests and porous-plate tests.

7. Capillary pressure relationships from mercury-injection tests differed significantly from those from other tests for all but one of the rock samples.

8. For video measurement of saturation profiles, the surface of observation must be open for flow. This open boundary conflicts with the boundary conditions of the one-dimensional radial numerical model used for matching the spinning-disk data. A two-dimensional model would provide means for avoiding this conflict, thus improving the quantitative value of the resulting relative permeabilities.

ACKNOWLEDGEMENTS

Support for Dr. Al-Omair was provided by Kuwait University. The centrifuge, computer, and video equipment were purchased in 1990 with funds generously provided by the Shell Foundation.

REFERENCES

1. Hagoort, J., "Oil Recovery by Gravity Drainage," *Soc. Pet. Eng. J*. (June 1980) **20**, 139-150.
2. Firoozabadi, A., Soroosh, H., and Hasanpour, G., "Drainage Performance and Capillary-Pressure Curves with a New Centrifuge," *J. Pet. Tech.* (July 1988) 913-919.
3. Chardaire-Riviere, C., Forbes, P., Zhang, J. F., Chavent, G., and Lenormand, R., "Improving the Centrifuge Technique by Measuring Local Saturations," Paper 24882 presented at the 1992 SPE Annual Technical Conference and Exhibition, Washington, D. C., Oct. 4-7.
4. Pohjoisrinne, T., Ruth, D., and Chen, Z. A., "A Capacitance Based Measurement System for Produced Fluids in a Pivoted or Horizontal Centrifuge," Paper SCA 9616 presented at the 1996 International Symposium of the Society of Core Analysts, Montpelier, France, September 8-10.
5. Al-Modhi, S., and Christiansen, R. L., "The 'Spinning Disk' Approach to Capillary Pressure Measurement with a Centrifuge Experiment," Paper 9834 in the Proceedings of the 1998 International Symposium of the Society of Core Analysts, The Hague, September 14-16.
6. Oyno, L., and Torsaeter, O., "Experimental and Numerical Studies of the Imbibition Mechanism," Presented at the 1990 North Sea Chalk symposium, Copenhagen, June 11-12. Also see Bolas, B., and Torsaeter, O.: "Theoretical and Experimental Study of the Positive Imbibition Capillary Pressure Curves Obtained from Centrifuge Data," Paper 9533 in the Proceedings of the 1995 International Symposium of the Society of Core Analysts, San Francisco, September 12-14.
7. Al-Omair, O. A., "Capillary Pressure and Relative Permeability in Centrifuge Experiments using the Spinning Disk Geometry," Ph. D. Thesis, Colorado School of Mines, 2001.
8. Christiansen, R. L., *Two-Phase Flow through Porous Media*, KNQ Engineering (2001) pp. 181-184.
9. Al-Omair, O., and Christiansen, R. L., "Measurement of Capillary Pressure by Direct Visualization of a Centrifuge Experiment," Paper 9838 in the Proceedings of the 1998 International Symposium of the Society of Core Analysts, The Hague, September 14-16.
10. Spinler, E. A., and Baldwin, B. A., "Capillary Pressure Scanning Curves by Direct Measurement of Saturation," Paper 9705 presented at the 1997 International Symposium of the Society of Core Analysts, Calgary, Alberta, Canada, September 7-10.